Design of Focusing Catadioptric Systems using Differential Geometry

Tobias Strauß
Institute of Measurement and Control Systems, Karlsruhe Institute of Technology (KIT), Karlsruhe, Germany

Keywords: Optical Design, Meridional Focus, Sagittal Focus, Astigmatism, Fermat'S Principle, Differential Geometry.

Abstract: In recent years catadioptric systems, consisting of lenses and mirrors, have gained increasing popularity for the task of environmental perception. However, focusing of such systems is a common problem as it is often not considered during the design process of the optical system.
This paper presents a novel approach to address focus in the design of optics with rotational symmetry. The approach does not only adress the construction of catadioptric systems but can also be used to calculate conventional optics. The approach is based on the calculation of the first order approximation of meridional and sagittal focus using differential geometry. Additional conditions like a single-viewpoint can be considered as well. The derived equations are combined to a set of ordinary differential equations that is used to calculate the shape of the optical system via numerical integration. The design concept has been verified by multi-chromatic ray tracing simulations.

1 INTRODUCTION

In the field of computer vision, environmental perception is an important task. For this, the possibility to capture a large field of view is often desirable. This can be performed using either ultra-wide-angle lenses or catadioptric systems consisting of both, lenses and mirrors (Benosman and Kang, 2001). For the task of capturing 360° panoramic images catadioptric systems are more advantageous as their field of view can be influenced in a wider range.

However, a big problem of today's catadioptric systems is their focusing as this is not considered during system design. Instead common designs only deal with the geometric mapping that describes the relation between image points and corresponding lines of sight (Hicks and Bajcsy, 2000; Stürzl and Srinivasan, 2010).

Neglecting wave effects, the light transport through an optical system can be described using light rays (Malacara and Malacara, 2003). The geometric mapping is defined by the *principal rays* which pass through the center of the aperture.

To adress focusing we have to deal with beams of rays. The rays of a single beam can be characterized as *meridional*, *sagittal* or *skew*. For systems with rotational symmetry, the rays that lie in the meridional plane spanned by the principal ray and the optical axis are called meridional rays. The sagittal rays are the rays that propagate in the sagittal plane that is perpendicular to the meridional plane and contains the principal ray (see Figure 1). The sagittal plane changes whenever the principal ray is reflected or refracted. Rays that are neither meridional nor sagittal are called skew.

In general the focus of the meridional rays differs from that of the sagittal rays and hence not all rays of a beam focus in one single point. This effect is called astigmatism (see Figure 2).

Baker and Nayar introduce the problem of defocus blur for catadioptric systems (Baker and Nayar, 1999). Swaminathan uses caustics to describe the focus (Swaminathan, 2007). However both approaches only deal with meridional focusing, leaving the sagittal focusing disregarded. Furthermore, the results are not used in a constructive way to improve the shape of the optic.

This paper presents an analytical way to calculate both meridional and sagittal focusing in a first order approximation using differential geometry and Fermat's principle.
A common approach when designing conventional optical systems is to use an iterative scheme of ray tracing simulations (Glassner, 1989) followed by draft rating using a so called merit function. In doing so, an initial system draft can be optimized until a minimum of the merit function has been found (Smith, 2004). However, this approach is time-consuming and the

Strauß T..
Design of Focusing Catadioptric Systems using Differential Geometry.
DOI: 10.5220/0004295300840089
In *Proceedings of the International Conference on Computer Vision Theory and Applications* (VISAPP-2013), pages 84-89
ISBN: 978-989-8565-47-1

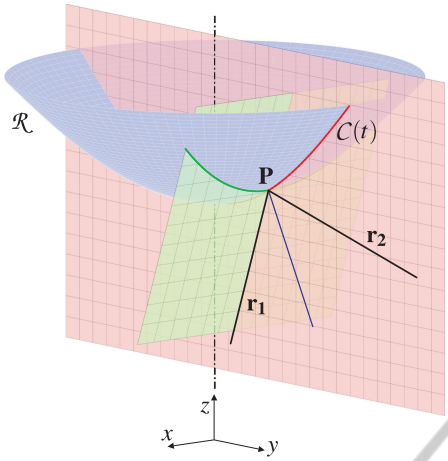

Figure 1: Reflection of a principal ray (black) at a surface of revolution $\mathcal{R}$ (blue) obtained by rotating a curve $\mathcal{C}(t)$ around the z-axis. $\mathbf{r_1}$ and $\mathbf{r_2}$ denote the direction vector of the incident and reflected ray. The surface's normal vector at the intersection point **P** is colored blue. The red plane is the meridional plane and one of the sagittal planes is shown in green. The red and green curve are the corresponding meridional and sagittal intersection curve respectively.

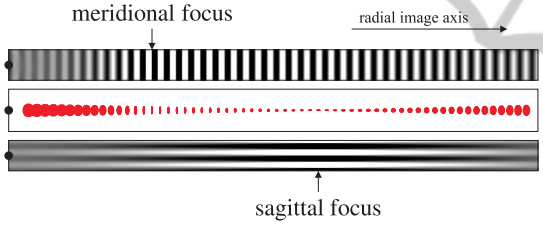

Figure 2: Simulated defocus blur of a single mirror optic attached to a conventional lens optic. The black dot in each sub-image marks the image center. The middle plot shows spots of several beams of rays along the radial image axis that can be understood as blur kernels dependent on the position. Related sample images with vertical and horizontal stripes visualize the defocus blur. At the meridional focus point the rays of one beam focus in radial direction, at the sagittal focus point they focus in circumferential direction.

quality of the optimal draft depends on the number of parameters used to describe the surfaces.

This paper presents a novel approach to design focusing optics that directly uses the analytical description of meridional and sagittal focus. In addition, relations for the geometric mapping can be considered - for example to ensure a single-viewpoint which is essential to be able to remap the image to other projection models without knowledge about the scene depth. All equations are combined to a system of ordinary differential equations describing the shape of the optical system. This ODE system can be solved quickly via numerical integration using standard methods like the Runge-Kutta methods without the need of ray tracing.

2 DESCRIPTION OF FOCUSING AT BOUNDING SURFACES

The analytical description of focusing at refracting and reflecting surfaces (referred to as bounding surfaces) is a central point of this paper. This section shows how the focusing characteristic of a beam of rays can be calculated using Fermat's principle. A first order approximation of a beam's focusing characteristic is given by its meridional and sagittal focus point. These focus points describe where rays focus that propagate within the meridional plane and sagittal plane respectively. They can be calculated in closed form using the intersection curve of surface and corresponding plane (see Figure 1).

2.1 Intersection of Bounding Surface and Meridional/Sagittal Plane

In the following, we examine a surface of revolution $\mathcal{R}$ which is defined by rotating a curve

$$\mathcal{C}(t) = (0, \rho(t), \zeta(t))^\mathsf{T} \tag{1}$$

around the z-axis (optical axis). To calculate the focusing induced by surface $\mathcal{R}$ using Fermat's principle, we need its intersection curves with meridional and sagittal plane. Without loss of generality we can assume $x = 0$ for the meridional plane. The intersection point of a principal ray and surface $\mathcal{R}$ can be expressed as $\mathbf{P} = \mathcal{C}(\tau)$. The normalized direction vectors of the incident and refracted principal ray at this point **P** are defined as $\mathbf{r_1} = (0, r_{1y}, r_{1z})^\mathsf{T}$ and $\mathbf{r_2} = (0, r_{2y}, r_{2z})^\mathsf{T}$ respectively. In the following, derivatives with respect to a certain parameter are marked with this parameter as a subscript, arguments are omitted for the sake of legibility, e.g. $\rho_t := \left.\frac{\partial \rho(t)}{\partial t}\right|_{t=\tau}$.

At each intersection point **P** we can define the meridional intersection curve and the sagittal intersection curve. The meridional intersection curve is equivalent to the curve $\mathcal{C}(t)$ itself. Its second order Taylor approximation at **P** with curve parameter u is given as

$$\mathcal{M}(u) = \mathbf{P} + \begin{pmatrix} 0 \\ \rho_t\, u + \frac{1}{2}\rho_{tt}\, u^2 \\ \zeta_t\, u + \frac{1}{2}\zeta_{tt}\, u^2 \end{pmatrix}. \tag{2}$$

The second order Taylor approximation of the sagittal intersection curve can be calculated using its mirror symmetry to the meridional plane and the Taylor series of $\mathcal{C}(t)$ at the intersection point. This yields:

$$\mathcal{S}(u) = \mathbf{P} + \begin{pmatrix} u \\ \frac{1}{2}\frac{r_{1y}\zeta_t}{\rho\left(r_{1z}\rho_t - r_{1y}\zeta_t\right)}\, u^2 \\ \frac{1}{2}\frac{r_{1z}\zeta_t}{\rho\left(r_{1z}\rho_t - r_{1y}\zeta_t\right)}\, u^2 \end{pmatrix}. \tag{3}$$

A detailed derivation is omitted due to lack of space.

2.2 Determination of Focus

Given the meridional and sagittal intersection curves, the corresponding focus points can be calculated using the laws of geometrical optics. Fermat's principle is a compact formulation of these laws which states that rays of light traverse the path of stationary optical path length (Hecht, 2001). The optical path length is defined as the product of geometrical length and refractive index of the surrounding medium.

In a first order approximation a beam of meridional rays neighboring the principal ray focuses in one point. This point is called the meridional focus point and lies on the straight line given by the principal ray. In an equivalent way a beam of sagittal rays focuses in the sagittal focus point. Thus, given the principal ray, the focus points can be expressed in terms of their distances to the surface.

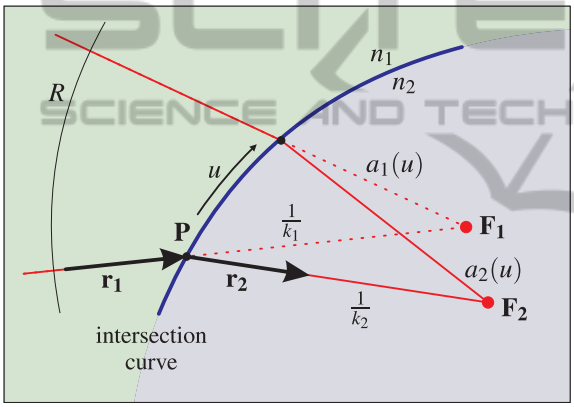

Figure 3: Sketch of the geometric relations used for the application of Fermat's principle. The sketch shows the planar meridional case. When dealing with sagittal focus, the rays do not lie within a plane and the problem has to be handled in 3-dimensional space.

To obtain a description that is also adequate for parallel rays (intersecting at infinity), we use the inverse Euclidean distance k between surface and focus point (see Figure 3). Applying Fermat's principle the value of k can be calculated depending on surface curvature and refractive indices of the adjoining media.

Under the assumption that the incident rays focus in the virtual focus point $\mathbf{F_1}$, they must all have the same phase (in terms of wave optics) at a circle of arbitrary radius R around $\mathbf{F_1}$. Hence it is sufficient to examine the optical path length between the intersection with such a circle and the focus point $\mathbf{F_2}$. This optical path length can be written as

$$w(u) = n_1 [R - a_1(u)] + n_2 \, a_2(u) \tag{4}$$

with the refractive indices n_1 and n_2 as well as the geometric distances $a_1(u)$ and $a_2(u)$.

For the principal ray to pass though point $\mathbf{F_2}$, Fermat's principle says that the corresponding optical path length must be stationary, so

$$w_u|_{u=0} \stackrel{!}{=} 0. \tag{5}$$

For the neighboring rays to pass through point $\mathbf{F_2}$, additionally condition (5) must be satisfied in a small neighborhood which is equivalent to

$$w_{uu}|_{u=0} \stackrel{!}{=} 0 \tag{6}$$

2.2.1 Meridional Focus

As the meridional focus points $\mathbf{F_{1m}}$ and $\mathbf{F_{2m}}$ lie on the principal ray, their positions can be expressed as

$$\mathbf{F_{1m}} = \mathbf{P} + \frac{1}{k_{1m}}\mathbf{r_1} \text{ and } \mathbf{F_{2m}} = \mathbf{P} + \frac{1}{k_{2m}}\mathbf{r_2} \tag{7}$$

with k_{1m} and k_{2m} denoting their inverse Euclidean distance to the intersection point.

Given the local quadratic approximation of the meridional intersection curve $\mathcal{M}(u)$ the optical path length for the neighboring meridional rays can be written as

$$\begin{aligned} w(u) = \; & n_1 R - n_1 \left| \mathcal{M}(u) - \mathbf{F_{1m}} \right| \\ & + n_2 \left| \mathcal{M}(u) - \mathbf{F_{2m}} \right|, \end{aligned} \tag{8}$$

where $|.|$ denotes the Euclidean norm, i.e.:

$$\begin{aligned} \left| \mathcal{M}(u) - \mathbf{F_{1m}} \right|^2 = & \left(\rho_t \, u + \frac{1}{2} \rho_{tt} \, u^2 - \frac{r_{1y}}{k_{1m}} \right)^2 \\ & + \left(\zeta_t \, u + \frac{1}{2} \zeta_{tt} \, u^2 - \frac{r_{1z}}{k_{1m}} \right)^2 \end{aligned} \tag{9}$$

With (7) the focus points lie on the principal ray. As the principal ray fulfills the laws of geometric optic condition (5) is satisfied by definition. To satisfy condition (6) we have to evaluate the second order derivative of (8) with respect to u at $u = 0$. After some longer arithmetic computation this yields:

$$\begin{aligned} & n_1 \left[k_{1m} \left(\rho_t \, r_{1z} - \zeta_t \, r_{1y} \right)^2 - \left(\rho_{tt} \, r_{1y} + \zeta_{tt} \, r_{1z} \right) \right] \\ & - n_2 \left[k_{2m} \left(\rho_t \, r_{2z} - \zeta_t \, r_{2y} \right)^2 - \left(\rho_{tt} \, r_{2y} + \zeta_{tt} \, r_{2z} \right) \right] \stackrel{!}{=} 0. \end{aligned} \tag{10}$$

This description of meridional focus is equivalent to the one gained using caustics (Swaminathan, 2007).

2.2.2 Sagittal Focus

As in the meridional case the sagittal focus points $\mathbf{F_{1s}}$ and $\mathbf{F_{2s}}$ lie on the principal ray. With the inverse Euclidean distances k_{1s} and k_{2s} their position can be expressed as

$$\mathbf{F_{1s}} = \mathbf{P} + \frac{1}{k_{1s}}\mathbf{r_1} \text{ and } \mathbf{F_{2s}} = \mathbf{P} + \frac{1}{k_{2s}}\mathbf{r_2}. \tag{11}$$

Given the local quadratic approximation of the sagittal intersection curve $\mathcal{S}(u)$, the optical path length for the neighboring sagittal rays can be expressed equivalent to (8). With the sagittal plane spanned by $\mathbf{r_1}$ and $\mathbf{e_x}$ condition (6) yields:

$$n_1\left[\frac{\zeta_t}{\rho\,(r_{1z}\rho_t - r_{1y}\zeta_t)} - k_{1s}\right] - n_2\left[\frac{\zeta_t\,(r_{1y}r_{2y} + r_{1z}r_{2z})}{\rho\,(r_{1z}\rho_t - r_{1y}\zeta_t)} - k_{2s}\right] \stackrel{!}{=} 0. \tag{12}$$

A full derivation is omitted due to lack of space. If we use the sagittal plane spanned by $\mathbf{r_2}$ and $\mathbf{e_x}$ to calculate the intersection curve and focusing, we get:

$$n_1\left[\frac{\zeta_t\,(r_{1y}r_{2y} + r_{1z}r_{2z})}{\rho\,(r_{2z}\rho_t - r_{2y}\zeta_t)} - k_{1s}\right] - n_2\left[\frac{\zeta_t}{\rho\,(r_{2z}\rho_t - r_{2y}\zeta_t)} - k_{2s}\right] \stackrel{!}{=} 0. \tag{13}$$

Using the law of geometrical optics, the equations (12) and (13) can be converted into each other by some arithmetic computation.

Note that ρ_{tt} and ζ_{tt} do not influence the sagittal focusing directly, but only its change dependent on t.

3 CONSTRUCTION SCHEME FOR OPTICAL SYSTEMS

The analytical description of the change of focus induced by a bounding surface given by (10) and (12) will now be used to design optical systems.

3.1 Parametric Description

In analogy to the last section, systems with rotational symmetry can be described with a set of planar curves $\mathcal{C}^i(t^i)$ with $i = 1 \ldots N$ corresponding to N bounding surfaces. One can choose a parametrization with a common curve parameter t for all curves $\mathcal{C}^i$ that is defined in a way that a certain value of t is related to a certain principal ray (see Figure 4). Such a parameterization is the basic step to describe the shape of an optical system using differential equations.

The parameterization gets unique by the definition of the incident principal rays. Here we use two planar curves $\mathcal{O}(t)$ and $\mathcal{A}(t)$, where the rays emanate from $\mathcal{O}(t)$ and pass through $\mathcal{A}(t)$.

To ensure the validity of parameterization the tangent vectors $\mathcal{C}_t^i(t)$ have to be chosen according to laws of geometrical optics. Each tangent vector depends only on the direction vectors of incident and reflected/refracted ray at the corresponding bounding

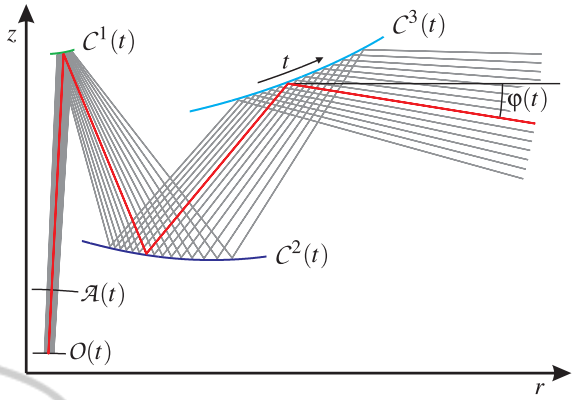

Figure 4: A set of planar curves $\mathcal{C}^i(t)$ can be used to describe the shape of an optical system with rotational symmetry. The curves $\mathcal{O}(t)$ and $\mathcal{A}(t)$ are used to describe the incident principal rays. $\varphi(t)$ denotes the exit angle of the principal rays.

surface. With functions $g^i(t)$ and $h^i(t)$ dependent on preceding, current and subsequent intersection point and scaling functions $p^i(t)$ we can write the tangent vectors $\mathcal{C}_t^i(t)$ as

$$\mathcal{C}_t^i(t) = (0, \rho_t^i, \zeta_t^i)^\mathsf{T} = p^i \cdot (0, g^i, h^i)^\mathsf{T}. \tag{14}$$

To determine the meridional intersection curve (2) we need to know the second order derivative of $\mathcal{C}^i(t)$ with respect to t. If we derive (14) w.r.t. t, we get:

$$\mathcal{C}_{tt}^i(t) = \begin{pmatrix} 0 \\ \rho_{tt}^i \\ \zeta_{tt}^i \end{pmatrix} = \begin{pmatrix} 0 \\ p_t^i g^i + p^i g_t^i \\ p_t^i h^i + p^i h_t^i \end{pmatrix}. \tag{15}$$

From a physical point of view, it is obvious that focusing is directly related to the curvature $\kappa^i(t)$. With (14) and (15) the curvature can be written as:

$$\kappa^i = \frac{\rho_t^i \zeta_{tt}^i - \rho_{tt}^i \zeta_t^i}{\left[(\rho_t^i)^2 + (\zeta_t^i)^2\right]^{\frac{3}{2}}} = \frac{g^i h_t^i - h^i g_t^i}{p^i \left[(g^i)^2 + (h^i)^2\right]^{\frac{3}{2}}}. \tag{16}$$

So in fact, the curvature is independent on p_t^i and we can set it to zero in (15). Note that g_t^i and h_t^i are dependent on $p^j(t)$, with $j \in \{i-1, i, i+1\}$.

The scaling function $p^1(t)$ is related to the curvature of curve $\mathcal{A}(t)$ and hence cannot be chosen freely. The functions g^N and h^N are related to the principal ray's exit angle $\varphi(t)$ and hence κ^N is influenced by $\varphi_t(t)$ as well. In summary, we now have a consistent description of a set of parametrized curves $\mathcal{C}^i(t)$ with common parameter t describing the path of the principal rays and a parameter vector

$$\mathbf{p}(t) = (p^2, \ldots, p^N, \varphi_t) \tag{17}$$

that influences the curvatures κ^i at every position t.

3.2 Propagation of Focusing Parameters

With (10) and (12) we are able to calculate the change of focusing at a single bounding surface. As the parameters k_m and k_s are defined relative to a certain intersection point $\mathbf{P}^i$ they have to be remapped to the next intersection point $\mathbf{P}^{i+1}$ before applying these equations for the next surface. In the following k^+ denotes the position of a focus point (meridional or sagittal) after this remapping. With the Euclidean distance s between the two reference points the propagation rule for the focus point description is:

$$\frac{1}{k^+} = \frac{1}{k} - s. \tag{18}$$

In order to propagate the change of sagittal focusing dependent on t, which is influenced by the surfaces' curvatures, we need the first order Taylor approximation of (18). With the linear approximations $k(t) \approx k_0 + k_t t$ and $s(t) \approx s_0 + s_t t$ we get:

$$k^+(t) \approx k_0^+ + k_t^+ t = \frac{k_0}{1 - s_0 k_0} + \frac{k_t + s_t {k_0}^2}{(1 - s_0 k_0)^2} t. \tag{19}$$

In an alternating manner of calculation of focusing at a bounding surface and propagation of the corresponding parameters to the next surface, we can calculate the object sided focusing parameters k_m, k_s and $k_{s,t}$. As already mentioned, k_s cannot be influenced directly via the surfaces' curvatures.

If we want to focus to infinity, we have to satisfy

$$k_m \stackrel{!}{=} 0 \text{ and } k_{s,t} \stackrel{!}{=} 0 \tag{20}$$

and in addition initially ensure that $k_s = 0$.

3.3 Single-viewpoint Condition

Additional conditions can be satisfied if the optical system design has enough degrees of freedom. For example we can demand a single-viewpoint, which means that all object sided principal rays intersect in one point $\mathbf{V} = (0, 0, v)^\mathsf{T}$ on the optical axis. A single-viewpoint is necessary if we want to remap a captured image to other projection models like the cylindrical projection without knowledge of scene depth. In order to satisfy the single-viewpoint condition, the exit angle $\varphi(t)$ must satisfy

$$\varphi(t) = \arctan\left(\frac{\zeta^N - v}{\rho^N}\right). \tag{21}$$

So we have to demand

$$\varphi_t(t) - \frac{\rho^N \zeta_t^N - (\zeta^N - v)\rho_t^N}{(\rho^N)^2 + (\zeta^N - v)^2} \stackrel{!}{=} 0. \tag{22}$$

3.4 Combined Root Finding Problem

With (20) and (22) we have three root finding problems that share a common parameter vector (17). The task of finding the corresponding parameter vector can be formulated as a multi-dimensional nonlinear least squares problem. To do so, we simply sum up the squared conditions. Such a nonlinear least squares problem can be solved using the Levenberg-Marquardt algorithm. Starting with an initial guess, this algorithm combines the Gauss-Newton algorithm with gradient descent to robustly find a local minimum. This local minimum should also be the global minimum with a sum of squared errors equal to zero. If the value at the local minimum is non-zero the initial root finding problem was not solved properly and we have not found a valid solution.

In general there exists more than one global minimum. A different minimum corresponds to a different shape of the final system and often comes along with a flipped inside-outside characteristic.

3.5 Final ODE System

The parameter vector (17) and the equations (14) and (22) define a set of differential equations for ρ^i, ζ^i and φ ($i = 2 \ldots N$). Given appropriate initial values, this system of ordinary differential equations can be solved via numerical integration with standard methods like the Runge-Kutta methods.

It has to be mentioned that a valid solution cannot be found for all sets of initial values. Sometimes it is simply not possible to satisfy the conditions or the solution's range of validity is not sufficiently large. However, for appropriate initial values the calculation of the optical system is very fast.

4 SIMULATION RESULTS

In the last section we presented a construction scheme for optical systems that directly considers meridional and sagittal focus as well as a single-viewpoint. This sections shows ray tracing results for a system draft that was calculated using this scheme. Ray tracing was performed using the spline interpolated numerical ODE solution. Material characteristics leading to the chromatic dispersion are considered as well.

As the construction scheme currently does not consider chromatic aberration we limited the refracting entry and exit surface in a way that the principal rays traverse these perpendicularly. To bundle the beams of rays on the image sensor we use two standard achromatic lenses (see Figure 5).

An additional aperture controls the amount of incoming light and higher order defocus blur.

The optical system was calculated for a $1/2.5$" sensor with 8.8 MP. This sensor has a pixel pitch of 1.55 μm. The partially mirrored main lens has a diameter of approximately 55 mm and was calculated to be manufactured from PMMA. The vertical field of view is approximately 17°.

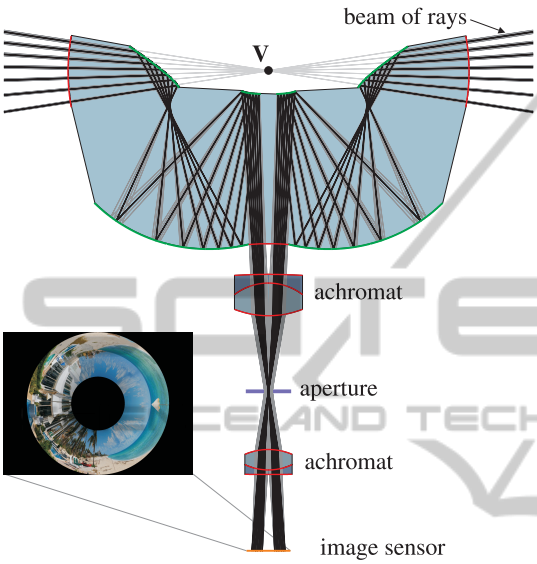

Figure 5: Optical design consisting of two standard achromatic lenses, an aperture and a mirror lens. The shape of the partially mirrored main lens was calculated using the presented design approach. Reflecting surfaces are colored green, refracting surfaces red. The principal ray of each beam of rays is shown in black, the other corresponding meridional rays are shown in gray color. All incident principal rays intersect in the single-viewpoint **V**.

Figure 6 shows the simulated defocus blur and chromatic aberration at different radial sensor positions. The spot sizes using an aperture diameter of 1 mm are even below the very small pixel size of 1.55×1.55 μm and let us expect a sharp image.

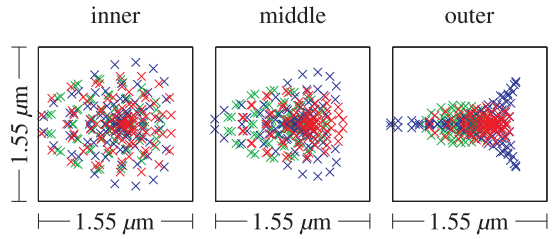

Figure 6: Simulated defocus blur of inner, middle and outer beams of rays relating to the image radius. Raytracing was performed for wavelengths of 500 nm (blue), 550 nm (green) and 650 nm (red). The colored crosses in each subplot show the sensor positions of different rays emanating from single object points at infinity.

5 SUMMARY AND CONCLUSIONS

In this paper we presented a novel approach to design focusing optics based on differential geometry. For this, an analytical description of meridional and sagittal focusing was derived using Fermat's principle. The approach considers focusing as well as geometric constraints. These are combined to a multi-dimensional root finding problem, whose solution is found using the Levenberg-Marquardt algorithm. In an iterative manner of solving the root finding problem and numerical integration the shape of the optical system is calculated.

A big advantage of this design approach compared to common approaches based on numerical parameter optimization is that the shape of the bounding surfaces is not restricted by a fixed number of parameters used to describe them.

An exemplary optical draft was analyzed by means of a multi-chromatic ray tracing simulation.

Future research will focus on the consideration of chromatic effects arising from refracting surfaces. This would overcome the limitation that refracting surfaces have to be traversed perpendicularly to avoid chromatic aberration.

ACKNOWLEDGEMENTS

The author would like to thank the Hans L. Merkle Foundation for funding this work.

REFERENCES

Baker, S. and Nayar, S. K. (1999). A theory of single-viewpoint catadioptric image formation. *International Journal of Computer Vision*, Vol. 35.

Benosman, R. and Kang, S. B. (2001). *Panoramic Vision: Sensors, Theory, and Applications*. Springer.

Glassner, A. S., editor (1989). *An Introduction to Ray Tracing*. Academic Press.

Hecht, E. (2001). *Optics*. Addison Wesley.

Hicks, R. A. and Bajcsy, R. (2000). Catadioptric sensors that approximate wide-angle perspective projections. *OMNIVIS 2000*.

Malacara, D. and Malacara, Z. (2003). *Handbook of Optical Design*. Marcel Dekker.

Smith, W. J. (2004). *Modern Lens Design*. McGraw Hill.

Stürzl, W. and Srinivasan, M. (2010). Omnidirectional imaging system with constant elevational gain and single viewpoint. *OMNIVIS 2010*.

Swaminathan, R. (2007). Focus in catadioptric imaging systems. *ICCV 2007*.